Cell, Vol. 99, 47–57, October 1, 1999, Copyright ©1999 by Cell Press

Targeted Mutagenesis of *Tsix* Leads to Nonrandom X Inactivation

Jeannie T. Lee,*†‡ and Naifang Lu*
*Department of Molecular Biology
Massachusetts General Hospital
Boston, Massachusetts 02115
†Department of Genetics
Harvard Medical School
Boston, Massachusetts 02114

Summary

During X inactivation, mammalian female cells make the selection of one active and one inactive X chromosome. X chromosome choice occurs randomly and results in *Xist* upregulation on the inactive X. We have hypothesized that the antisense gene, *Tsix*, controls *Xist* expression. Here, we create a targeted deletion of *Tsix* in female and male mouse cells. Despite a deficiency of *Tsix* RNA, X chromosome counting remains intact: female cells still inactivate one X, while male cells block X inactivation. However, heterozygous female cells show skewed *Xist* expression and primary nonrandom inactivation of the mutant X. The ability of the mutant X to block *Xist* accumulation is compromised. We conclude that *Tsix* regulates *Xist* in *cis* and determines X chromosome choice without affecting silencing. Therefore, counting, choice, and silencing are genetically separable. Contrasting effects in XX and XY cells argue that negative and positive factors are involved in choosing active and inactive Xs.

Introduction

In mammals, X inactivation ensures that female and male cells achieve dosage equivalence of X-linked genes (Lyon, 1961). Before implantation, both X chromosomes are active in XX female embryos, but one must be transcriptionally silenced at the time pluripotent cells differentiate along increasingly restricted embryonic lineages (Epstein et al., 1978; Kratzer and Gartler, 1978; Monk and Harper, 1979). At the peri-implantation stage, an X chromosome counting mechanism determines the X:autosome ratio and permits X inactivation only when the X chromosome number exceeds one in a diploid nucleus. Each XX cell then makes the epigenetic choice to keep one X active and to inactivate the other. At present, it is unclear whether choosing involves selecting the future active or inactive X. In principle, three types of mechanisms may be used (Ohno, 1969; Eicher, 1970; Lyon, 1971, 1972; Drews et al., 1974; Gartler and Riggs, 1983). In the first, the default state during cell differentiation is to remain active and cells must produce a positive factor to inactivate additional Xs. Alternatively, the default state is to be inactivated and cells protect one X from inactivation through a "blocking factor" (negative factor). Finally, the choice of active and inactive X may involve purposeful selection of each through both a negative and a positive factor.

A blocking factor mechanism has gained considerable support (Lyon, 1996; Brockdorff, 1998). In this class of models, a diploid cell produces a blocking factor that marks the future active X by "blocking" its inactivation control center (*Xic*). The remaining X(s) is unprotected and undergoes inactivation by default. These models are consistent with a large body of genetic evidence and explain why diploid cells follow the "n − 1" rule: XY cells do not undergo X inactivation, XX cells inactive one X, XXX cells inactive two, and XXXX cells inactivate three. However, models proposing blocking factors are not mutually exclusive with those proposing positive factors. Indeed, recent genetic evidence suggests that both negative and positive factors may work together to choose active and inactive Xs, respectively (Marahrens et al., 1998).

Molecular models for the choice mechanism must take into account that, in an XX cell, the two Xs have an equal chance of being inactivated and the decision is mitotically stable (McMahon et al., 1983). However, epigenetic and genetic factors can influence choice. For example, in metatherian mammals (e.g., kangaroos [Cooper et al., 1971]) and in the extraembryonic tissues of some eutherian mammals (e.g., mice [Takagi and Sasaki, 1975]), the paternal X chromosome is imprinted and always undergoes inactivation. In mice, choice can be influenced by the *Xce* (X controlling element), such that the X chromosome with a strong *Xce* allele is more likely to remain active (Cattanach and Papworth, 1981). While an equivalent *Xce* locus has not been found in humans, skewed X inactivation patterns have been associated with a promoter mutation in *XIST* (Plenge et al., 1997).

The past decade has brought greater molecular understanding of the X inactivation process. X inactivation requires a master genetic switch called the "X inactivation center" (*Xic*; reviewed by Rastan and Brown, 1990), a multifunctional locus carrying elements for counting, choosing, and silencing (Lee et al., 1996, 1999b; Herzing et al., 1997). The silencing function requires *Xist*, an *Xic* gene that produces a large untranslated RNA which "coats" the inactive X (Brockdorff et al., 1992; Brown et al., 1992; Clemson et al., 1996). Knocking out *Xist* expression abolishes silencing without disrupting counting (Penny et al., 1996), suggesting that *Xist* acts downstream of counting and is likely a genetic target of factors involved in counting and choosing. Dynamic changes in *Xist* expression mark the initiation of X inactivation (Panning et al., 1997; Sheardown et al., 1997). Prior to the onset of X inactivation, both male and female cells show basal *Xist* expression. During differentiation, *Xist* is turned off in male cells. In female cells, the two X chromosomes adopt opposite fates: on the future active X, *Xist* is turned off; on the future inactive X, *Xist* is upregulated and the RNA accumulates along the

‡To whom correspondence should be addressed (e-mail: lee@molbio.mgh.harvard.edu).

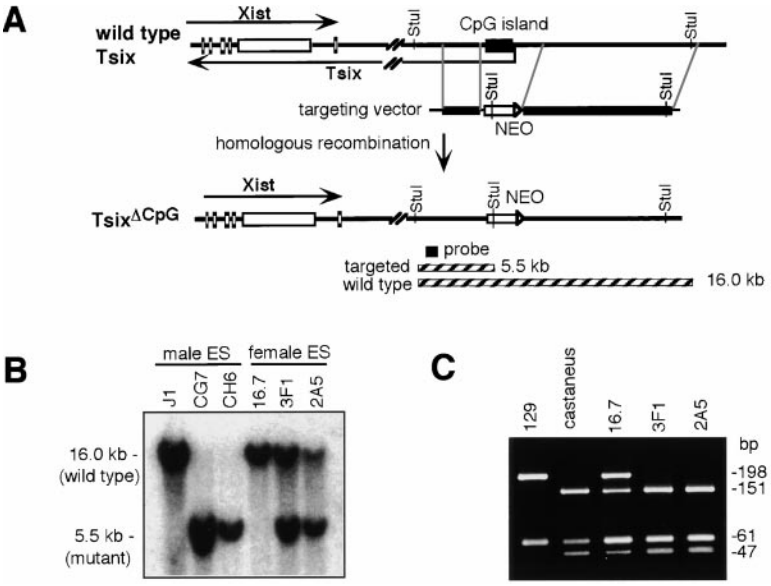

Figure 1. Targeted Mutagenesis of *Tsix*

(A) Scheme for generating $Tsix^{\Delta CpG}$.

(B) Southern analysis of mutant male (CG7, CH6) and mutant female (3F1, 2A5) DNA cut with StuI. The probe was a 0.67 kb fragment external to the targeting vector and detected StuI fragments as depicted in (A).

(C) The 129 allele was targeted in both female clones (3F1, 2A5), as indicated by absence of a 129-specific MnlI restriction pattern (N. Stavropoulos, unpublished observation). A 259 bp fragment (12,553–12,812 bp downstream of *Xist* exon 6) partially lying within ΔCpG was PCR amplified and digested with MnlI. The *M. castaneus* allele contained an additional MnlI site and gave rise to fragments of 151, 61, and 47 bp, while the 129 allele gave rise to fragments of 198 and 61 bp.

chromosome in *cis*, perhaps enabling recruitment of silencing proteins.

Transgenic studies have provided clues to minimal sequence requirements for *Xist* regulation. Aspects of this regulation have been recapitulated on autosomes carrying *Xist* and various flanking sequences (Lee et al., 1996, 1999b; Herzing et al., 1997). In an 80 kb *Xic* transgene, deleting a 30 kb sequence upstream of *Xist* abolished *Xist* upregulation, suggesting the presence of a positive *Xist* regulator (Lee et al., 1999b). A repressive element downstream of *Xist* is implicated by constitutive *Xist* expression and primary nonrandom X inactivation in a 65 kb knockout (Clerc and Avner, 1998). Finally, a positive regulator for X chromosome choice has been suggested by an internal *Xist* deletion that leads to primary nonrandom X inactivation (Marahrens et al., 1998). Thus, the control of X inactivation may depend on a series of molecular switches involving both positive and negative factors.

The antisense gene, *Tsix*, was recently discovered downstream of *Xist* as a candidate *Xist* regulator (Lee et al., 1999a). Like *Xist* RNA, *Tsix* RNA is exclusively nuclear and is dynamically regulated during X inactivation. Before X inactivation, *Tsix* is biallelically expressed but becomes monoallelically expressed at the onset of X inactivation, marking only the future active X and therefore raising the possibility that *Tsix* blocks *Xist* accumulation. To test this hypothesis, we carried out targeted mutagenesis of murine *Tsix* in XX female and XY male cells. Below, we describe their effects on X chromosome counting, choice, and silencing and deduce a model incorporating a role for *Tsix* in the epigenetic regulation of X chromosome choice.

Results

Targeted Mutagenesis of *Tsix* ($Tsix^{\Delta CpG}$)

Because mouse embryonic stem (ES) cells have been established as in vitro models of X inactivation (Rastan and Robertson, 1985; Lee et al., 1996; Penny et al., 1996; Clerc and Avner, 1998), we selected male and female ES cells to study effects of knocking out *Tsix*. Undifferentiated ES cells are naive with respect to X inactivation but undergo counting, choosing, and silencing when placed under differentiation conditions. Since the *Xic* may be genetically complex, we minimized disturbance to the region by deleting only 3.7 kb of *Tsix* (Figure 1A). This deletion ($Tsix^{\Delta CpG}$) encompassed the *Tsix* CpG island, transcriptional start sites, and 1.4 kb of upstream sequence containing the putative promoter. We introduced the mutation into the male ES cell line, J1 (Li et al., 1992), and analyzed two independent clones, CG7 and CH6 (Figure 1B). We also targeted one X chromosome in the female ES cell line, 16.7, and analyzed two independent clones, 3F1 and 2A5 (Figure 1B). 16.7 carried two stable X chromosomes, one each of 129 and *Mus castaneus* origins. As judged by fluorescence in situ hybridization (FISH) with X-linked probes, 3F1 and 2A5 were karyotypically stable (>90% 40XX). The 129 allele was targeted in both (Figure 1C).

To exclude potential artifacts due to insertion of a *neo* cassette at the site of ΔCpG, we generated subclones of CG7 and 3F1 in which *neo* was removed by Cre-mediated recombination at flanking loxP sites. In the following experiments, neo^+ and neo^- clones were studied in parallel and, because they manifested no differences, only neo^+ clones are further described below.

Effects of ΔCpG on *Tsix* and *Xist* Expression in Undifferentiated Cells

To determine whether the ΔCpG mutation abolished *Tsix* expression, we examined antisense transcription in undifferentiated ES cells at five positions across the 40 kb *Tsix* region (Figure 2A). In mutant male cells, antisense transcription was undetectable by strand-specific RT–PCR (30-cycle) and RNA FISH at any position tested, in contrast to that in normal male cells (Figures 2B and 2C). CG7 and CG6 showed identical results. In mutant female cells, no antisense RNA was visible on the targeted chromosome at any of five positions, but it was

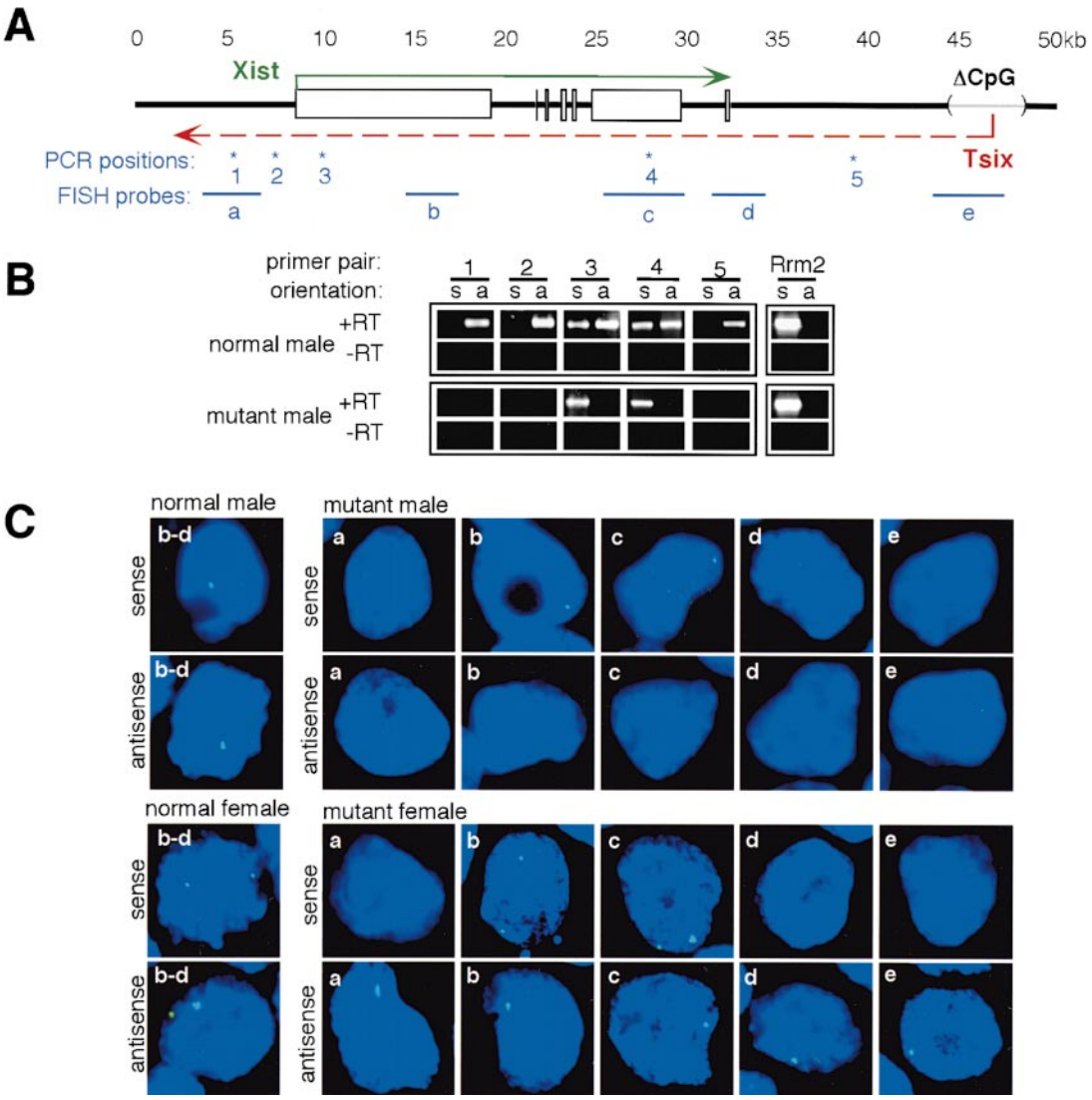

Figure 2. Effects of ΔCpG on *Tsix* and *Xist* Expression in Undifferentiated ES Cells

(A) Map of the *Xic*.

(B) Strand-specific 30-cycle RT–PCR at indicated positions of normal and mutant male ES cells. "s" (sense) and "a" (antisense) refer to the orientation of detected transcript. *Rrm2*, ribonucleotide reductase M2.

(C) Strand-specific RNA FISH in normal and mutant male and female ES cells using probes (*a*–*e*) as indicated by white letters in each panel. Pooled probes *b*–*d* were used for normal cells. At least 100 nuclei were examined for each probe–cell line combination. An experiment was scored as positive only if >80% of nuclei exhibited signals. Signal specificity was confirmed by colocalization to *Xic* probes (data not shown).

visible on the normal X in the same nucleus by RNA FISH (Figure 2C). The targeted and normal Xs were distinguished by hybridization to *Xic*-specific DNA sequences (e.g., ΔCpG deletion probe; see below). The size, intensity, and quality of antisense signals on the normal chromosome were similar to those seen in normal female cells. 3F1 and 2A5 showed identical results. Thus, ΔCpG affected *Tsix* expression only in *cis*. ΔCpG's effect was similar at all positions tested, supporting the idea that *Tsix* encodes a single large transcript rather than multiple smaller RNAs. Although ΔCpG deletes the previously mapped *Tsix* transcriptional start sites (Lee et al., 1999a), minor transcriptional start sites could be present further upstream, since weak antisense RT–PCR bands were variably present at positions 1 to 5 when 5–10 additional cycles were included (data not shown). It is unclear whether this represented low-level residual transcription due to minor and/or cryptic promoters or were instead artifacts of overcycling PCR conditions, especially because antisense signals were not detected by RNA FISH on ΔCpG chromosomes.

In undifferentiated cells, *Xist* RNA did not accumulate on the mutant X in male (CG7, CH6) and female (3F1, 2A5) mutants. Five positions were examined by sense-specific RNA FISH (Figure 2C). Sense transcription was observed at positions *b* and *c*, and variably at *d* but not at *a* or *e*, consistent with previous analysis (Lee et al., 1999a). In mutant and normal cells, *Xist* RNA was always more difficult to detect than *Tsix* RNA and required signal amplification. In mutant male nuclei, we observed

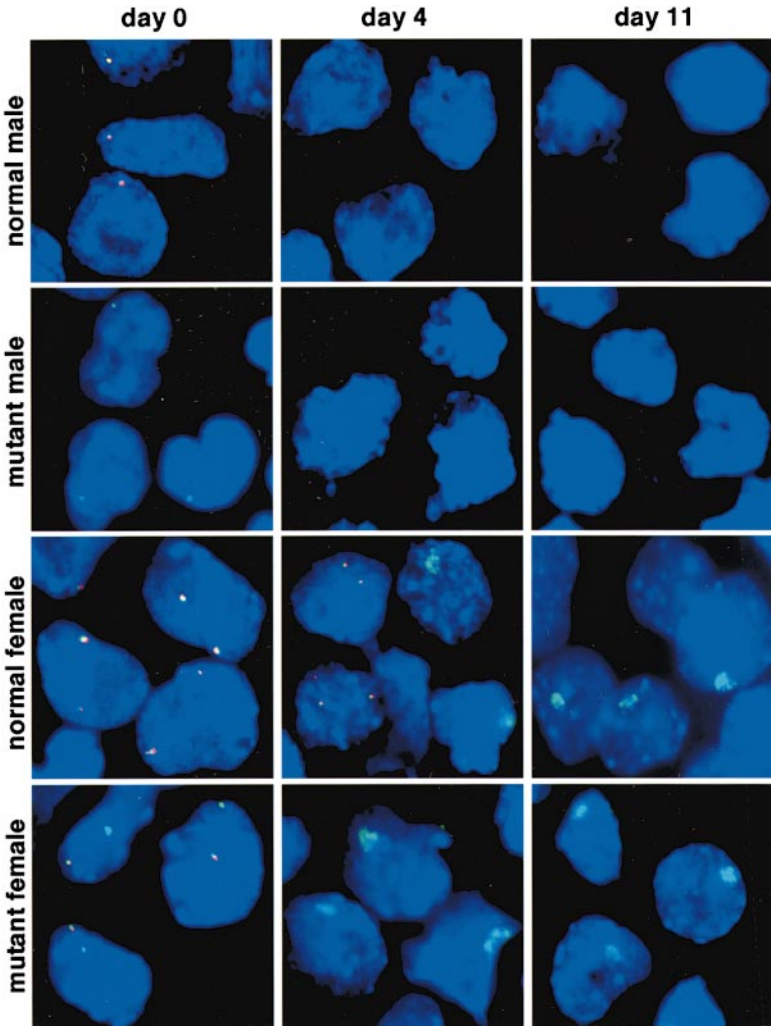

Figure 3. ΔCpG Did Not Abolish Chromosome Counting

Xist (green) and *Tsix* (red) expression in ES (day 0) or EB (day 4 and day 11) cells was assessed by RNA FISH using strand-specific probe cocktail *b–d* (Figure 2). Two hundred nuclei were examined for each probe–cell line combination.

single weak pinpoint signals that were similar to those seen in normal male nuclei. In mutant female nuclei, we found comparable signals on targeted and wild-type X chromosomes, both similar to those of normal female nuclei. Strand-specific RT–PCR confirmed sense transcription at positions 3 and 4 but not at 1, 2, or 5 (Figure 2B).

Tsix$^{\Delta CpG}$ Does Not Affect X Chromosome Counting

To examine the integrity of counting, we differentiated mutant ES cells into embryoid bodies (EB) and asked whether XX and XY cells properly switched on or off X inactivation. Since *Xist* upregulation is a marker for X inactivation, aberrant counting could be manifested by inappropriate *Xist* upregulation in XY cells, biallelic *Xist* upregulation in XX cells, or no upregulation at all in XX cells. Such aberrant counting might be expected to result in massive cell death due to lack of dosage compensation. We used two-color RNA FISH to examine *Xist* and *Tsix* expression simultaneously in female and male mutants (Figure 3).

Mutant female cells (3F1, 2A5) behaved similarly to normal female cells. Undifferentiated (day 0) cells expressed biallelic basal *Xist* ($>$90%, n = 200), and differentiating cells demonstrated increasing proportions of monoallelic high-level *Xist* ($\sim$75% of nuclei on day 4, $>$90% on day 11; n = 200 each). Biallelic high-level *Xist* expression was not found in either mutant or normal lines. In mutant female cells, the wild-type *Tsix* allele persisted briefly during differentiation and was repressed between days 4–11 with kinetics similar to that of normal female cells. Normal and mutant EB cultures differentiated equally well, as judged by rate of EB growth and rate at which various cell morphologies appeared (refer to Figure 6). Cell death was not elevated in mutant female lines (data not shown). These results indicated that dosage compensation was properly switched on in mutant female cells.

Mutant male EB (CG7, CH6) also behaved identically to normal male EB. Low-level *Xist* was seen in $>$95% of mutant nuclei (n = 200) on day 0 and was repressed between day 4 (*Xist* RNA in $\sim$30%, n = 200) and day 11 of differentiation (*Xist* RNA in $<$5%, n = 200). These results were similar to those of normal male EB. *Tsix* RNA was not seen in mutant cells at any time (0%, n = 200), while *Tsix* persisted briefly in normal male nuclei and disappeared completely by day 11. Mutant male EB showed normal growth rates and differentiation potential (refer to Figure 6). Massive cell death did not take place at any time.

Normal *Xist* expression patterns and cell survival in

A

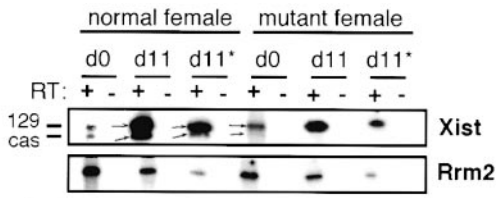

Xist	normal female		mutant female	
	d0	d11	d0	d11
129	52	1700	135	2250
cas	48	300	15	0
fold-upregulation:		22x		15x

B

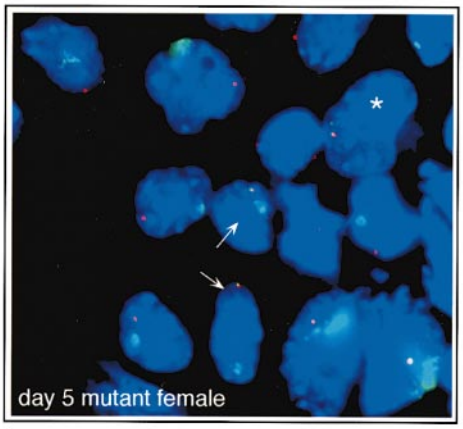

C

mutant female EB	Xist RNA colocalization: X^{mut} (%)	X^{wt} (%)	both	n†
day 2	100 (98.0)	2 (2.0)	0 (0.0)	102
day 5	196 (97.5)	5 (2.5)	0 (0.0)	201

† only nuclei with high level Xist RNA were scored.

Figure 4. Nonrandom Choice of *Xist* Expression in Mutant Female EB Cells

(A) The clonal 16.7 cell line did not show predetermined choice of *Xist* allele, as both 129 and *M. castaneus* (cas) alleles could be upregulated. Allelic-specific quantitative *Xist* RT–PCR was performed on day 0 (d0) and day 11 (d11) 16.7 and 2A5 EB cells. The 129 product was 227 bases, and *M. castaneus* was 224 bases. d11* was a 4-fold dilution of d11. The table summarizes relative levels of *Xist* representative of two independent experiments. All *Xist* values were normalized to *Rrm2*. The extent of total *Xist* upregulation from day 0 to day 11 is indicated below normal and mutant samples.

(B) Two-color simultaneous RNA-DNA FISH of day 5 mutant female cells. *Xist* RNA was detected by sense probes *b–d* (see Figure 2; green signals), and the wild-type X chromosome was detected by the ΔCpG probe (red). As in normal female cultures, cells in several stages of differentiation are evident at day 5 (Lee et al., 1999a): asterisk, undifferentiated cell with low-level *Xist* RNA from normal (green *Xist* RNA signal colocalizing with red DNA signal) and mutant X chromosome (green *Xist* signal only); arrows, differentiating cells in "transitional" stage with high-level *Xist* from mutant chromosome and low-level *Xist* RNA still present on normal chromosome; most other cells in the field are "mature forms" with high-level *Xist* expression exclusively from the mutant chromosome (lack of colocalizing red DNA signal).

(C) Summary of allelic *Xist* expression in day 2 or day 5 mutant female EB cells (3F1, 2A5) as assessed by RNA-DNA FISH. Only cells with high-level *Xist* expression were scored.

differentiating cells suggested that mutant male cells properly blocked X inactivation and mutant female cells appropriately inactivated one X. These results argued that the counting mechanism was not disrupted by ΔCpG.

Biased *Xist* Expression in Female Mutants

Normal XX female cells stochastically inactivate either the paternally or maternally inherited X. In the parental 16.7 female line, this is manifested by the ability of both the *M. castaneus* and 129 *Xist* alleles to be upregulated during differentiation (Figure 4A). Expression from the 129 allele was more abundant, consistent with 129's lower *Xce* strength (Xce^a) relative to that of *M. castaneus* (Xce^c) (Cattanach and Rasberry, 1994). Importantly, high-level expression of both *Xist* alleles in 16.7 demonstrated that X chromosome choice was not predetermined in the parental ES line. If the role of *Tsix* were to block *Xist* upregulation, one possible outcome of deleting *Tsix* would be constitutive *Xist* expression in *cis* and biased X chromosome choice.

Here, we used quantitative strand- and allele-specific RT–PCR to examine *Xist* upregulation during differentiation (Figure 4A). The steady-state levels of *Xist* RNA at day 11 and the magnitude of *Xist* upregulation from day 0 to day 11 (>15-fold) were similar in normal and mutant female cells. However, mutant cells showed complete skewing of *Xist* expression toward the 129 species (100% of total RNA). The results of RNA-DNA FISH confirmed these findings (Figures 4B and 4C). In this assay, targeted and normal chromosomes were distinguished by hybridization to the ΔCpG sequence that specifically detected the wild-type X. In female mutants, *Xist* was almost exclusively upregulated from the targeted chromosome (>97.5%). In rare nuclei (<2.5%), the ΔCpG DNA probe was coincident with high-level *Xist* RNA. Because the DNA signal was often at the periphery of the *Xist* RNA domain, these rare cells could represent chance juxtaposition of normal and targeted chromosomes rather than true expression from the normal X. These results indicated that a deficiency of *Tsix* led to an extreme, if not complete, bias of *Xist* upregulation from the mutant chromosome.

Quantitative RT–PCR also showed that ΔCpG exerted some effect on *Xist* expression even before differentiation in mutant female cells (Figure 4A). On day 0, the steady-state *Xist* levels were approximately 50% greater in mutant female cells than in normal female cells. Moreover, *Xist* expression was skewed toward the 129 allele in mutant cells (90% of total in mutants, compared to 52% in normal cells). These observations suggested that a deficiency of *Tsix* increased the steady-state level of *Xist* RNA in *cis*. Intriguingly, however, while *Xist* levels were mildly elevated in mutant cells, RNA FISH revealed no accumulation of *Xist* transcripts over the mutant chromosome (Figures 2 and 3).

Primary Nonrandom X Inactivation In Vitro

To test whether biased *Xist* expression resulted in nonrandom X inactivation, we examined nascent transcription of *Pgk1* (3 cM telomeric to the *Xic*) and *Mecp2* (13 cM centromeric to the *Xic*), two X-linked genes that are normally subject to X inactivation. ΔCpG did not affect the ability of *Xist* RNA to spread along the entire mutant

A

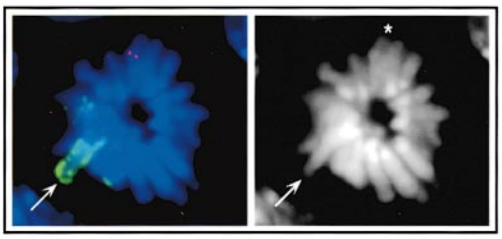

B

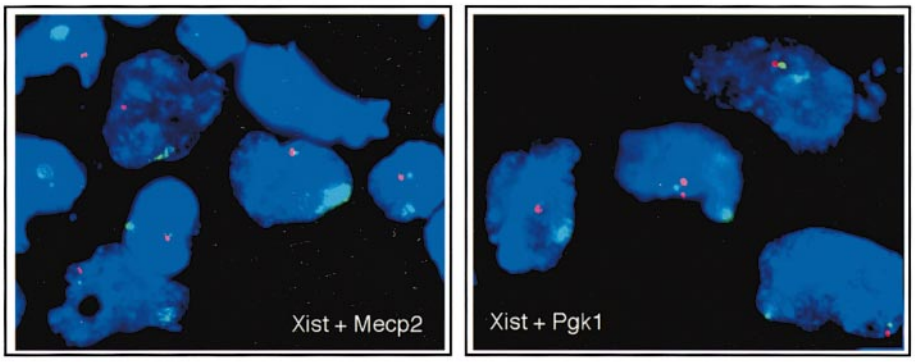

C

	Pgk1 or Mecp2 RNA colocalization with:			#nuclei n†
	X^{mut} (%)	X^{wt} (%)	both (%)	
Pgk1	3 (1.2%)	259 (98.8%)	0 (0%)	262
Mecp2	0 (0%)	251 (98.4%)	4 (1.6%)	255

† Only cells with high level Xist RNA and detectable Pgk1 or Mecp2 expression were scored.

Figure 5. Long-Range Silencing of *Pgk1* and *Mecp2* on the Mutant X Chromosome

(A) *Xist* RNA (green) decorated the mutant X chromosome (arrow), as demonstrated by RNA-DNA FISH of mitotic chromosomes from mutant female EB cells (day 4). Wild-type X is marked by the ΔCpG probe (red; asterisk). Chromosomes were counterstained with DAPI (right panel).

(B) Two-color RNA FISH of mutant female EB cells (day 2) using probes for *Pgk1* or *Mecp2* RNA (red) and *Xist* RNA (green). Note that *Pgk1* and *Mecp2* RNA signals were not precisely in register with low *Xist* signals because they are located 3 and 13 cM away from *Xist*. Chromosomes with high *Xist* levels were inferred to be mutant (see Figure 4).

(C) Summary of results from day 2–6 EB cells in 3F1 and 2A5 mutant female lines. The two lines behaved identically. *Pgk1* RNA was detected in 40%–50% of all nuclei and *Mecp2* RNA in >85%. Only those cells with high-level *Xist* RNA and detectable *Pgk1* or *Mecp2* RNA were counted.

X (Figure 5A). *Pgk1* nascent RNA was visualized in 40%–60% of normal and mutant nuclei from days 2 to 6 (n = 100 each). *Mecp2* nascent RNA was seen in >85% of normal and mutant nuclei (n = 100 each). To determine the allele of transcription, RNA FISH for *Xist* and *Pgk1* or *Mecp2* was performed simultaneously (Figure 5B). As the *Xist*-coated domain marks the mutant X (Figure 4), the origin of *Pgk1* or *Mecp2* RNA was deduced from its localization relative to the large *Xist* domain. In virtually all cells with visible *Pgk1* and *Mecp2* nascent RNA, the transcript was located outside the *Xist* RNA territory (Figures 5B and 5C). Thus, high *Xist* expression on the mutant X correlated with repression of two X-linked genes in *cis*, indicating that ΔCpG did not affect silencing. ΔCpG's effect was instead manifested as highly skewed inactivation of the mutant X chromosome.

Because the mutant X was distinguishable from the normal X by a *Pgk1* promoter–driven *neo*-resistance marker, we reasoned that nonrandom inactivation of the mutant X would be reflected in progressive G418 sensitivity of differentiating EB cultures as X inactivation proceeded to completion. Indeed, while all male and female cultures grown without G418 were equally healthy (beating heart structures, vessels, and neurons were evident between days 11–21), mutant female EBs (3F1, 2A5) grown in G418-containing media underwent massive cell death from days 8 to 15 and did not form recognizable structures. At 21 days, the difference in cell mass between +G418 and −G418 mutant female cultures was $\sim 10^2$ live cells (+G418) versus $>10^7$ live cells (−G418), as assessed by Trypan blue staining. Rare live cells were expected in +G418 cultures, since some cells might have remained undifferentiated. Normal male and female controls underwent massive cell death between days 6 and 10. A slight delay in mutant cell death was not unexpected, as the *neo* product expressed by undifferentiated cells likely persisted for some time during differentiation due to a lag in protein turnover. These results further demonstrated an extreme bias toward inactivating the mutant chromosome. In contrast to female mutants, male mutants (CG7, CH6) survived G418 selection to 21 days. Mutant male cultures differentiated normally and showed no anomalous cell death, with +G418 and −G418 cultures supporting $>10^7$ live cells each. This female-specific lethality indicated that *neo* repression was not due to its location in the *Xic* or to differentiation per se. Instead, it implicated nonrandom X inactivation as the cause.

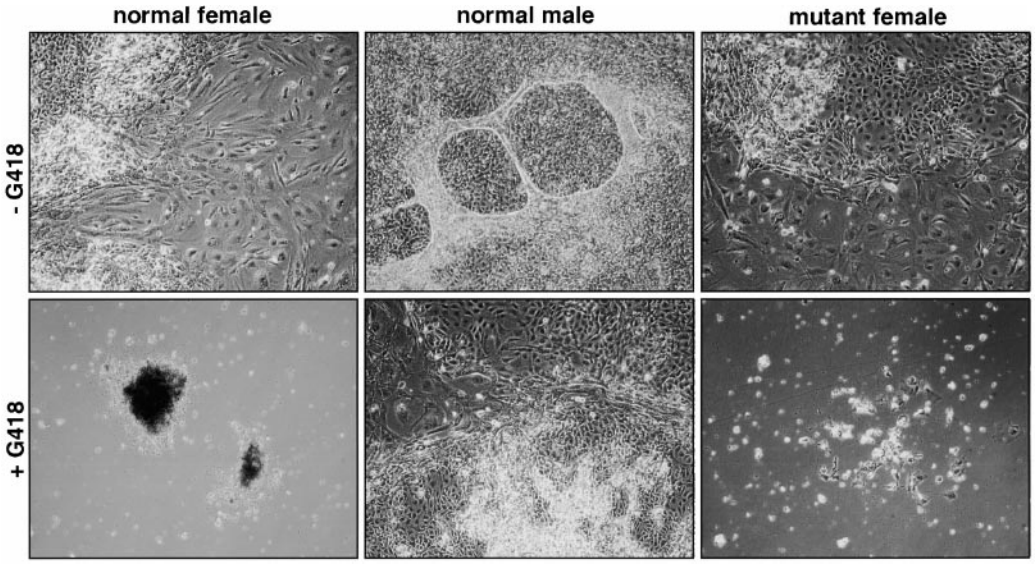

Figure 6. Primary Nonrandom X Inactivation In Vitro: Skewed Inactivation of the *neo* Marker in Mutant Female Cells

Normal female, mutant male (CG7 shown), and mutant female (2A5 shown) EB cells were grown in suspension culture for 4 days without drug, then split evenly between dishes containing no drug or 0.5 mg/ml G418 (in DME +10% FCS). EB cells attached to plates on day 4 and were grown in differentiation conditions up to day 21.

In principle, nonrandom X inactivation could be due to primary or secondary causes. Primary nonrandom X inactivation would result if ΔCpG destroyed the choosing mechanism—either *Tsix* RNA or a binding site for the putative blocking factor—so that only the wild-type X could be selected as the active X. Primary nonrandom X inactivation would also result if ΔCpG did not directly destroy the blocking factor site but affected the ability to bind the site irreversibly. The blocking factor could be in equilibrium between the two Xs and commit to one X only after *Tsix* expression is engaged in *cis* (via positive feedback regulation).

Secondary nonrandom X inactivation would arise if *Tsix* were required to block *Xist* upregulation but were not part of the choosing mechanism per se. Cells would still be able to choose between the wild-type and mutant Xs. However, choosing the mutant as the active X (and therefore the wild type as the inactive X) would be lethal due to a *cis* deficiency of *Tsix*, a state that would lead to double *Xist* upregulation and X inactivation. Thus, in this case, the observed nonrandom pattern of inactivation would be a secondary consequence of selective cell loss. The data did not support a secondary mechanism, since biallelic high-level *Xist* expression was not seen during EB differentiation and no excess cell death was observed (Figures 3, 4, and 6). Our results argued instead that a deficiency of *Tsix* led to primary nonrandom X inactivation due to loss of X chromosome choice.

Nonrandom X Inactivation In Vivo

We generated chimeric mice from mutant ES cells to confirm above findings in an organismic context. Mutant male cells gave rise to healthy chimeras (>90% chimerism), consistent with appropriate blocking of X inactivation despite a *Tsix* deficiency. Mutant female cells gave rise to healthy chimeras (60%–90% chimerism), underwent X inactivation appropriately, but demonstrated a highly skewed pattern of X inactivation (Figures 7A and 7B). RNA-DNA FISH showed that the mutant X was inactivated in over 96% of primary fibroblast cells isolated from two independent mice. Rare cells (<4%) showed apparent colocalization of ΔCpG DNA and *Xist* RNA signals. Because the DNA signal was often located at the periphery of the RNA domain, colocalization may represent chance juxtaposition of two Xs rather than true upregulation from the wild-type X. (N.B., Primary cultures contained mixtures of host [normal female] and ES-derived mutant female cells, but host and ES-derived fibroblasts were distinguished by the number of ΔCpG hybridization signals, which reflects the number of normal X chromosomes. Host cells in both chimeras were female.)

Skewed X inactivation in vivo was further confirmed by testing somatic cells for inactivation of the *neo*-resistance marker. Primary mutant female fibroblasts demonstrated striking sensitivity to G418 (Figure 7C). Like their EB counterparts in vitro, mutant female fibroblasts failed to grow in the presence of G418. Massive cell death was evident after 4 days in both mutant female and normal female cultures. Inviability was specifically related to repression of *neo* on the mutant X, because introduction of an exogenous *neo* gene by retroviral transfection completely restored G418 resistance (data not shown). Additionally, mutant male primary fibroblasts derived from CG7 and CH6 chimeras were fully *neo* resistant (Figure 7C), arguing against a position effect on the *neo* cassette. These data demonstrated that the ΔCpG phenotype observed in vitro was recapitulated during embryogenesis in vivo.

Discussion

We have carried out targeted deletion of the 5′ CpG-rich domain of *Tsix*. ΔCpG resulted in deficient expression of

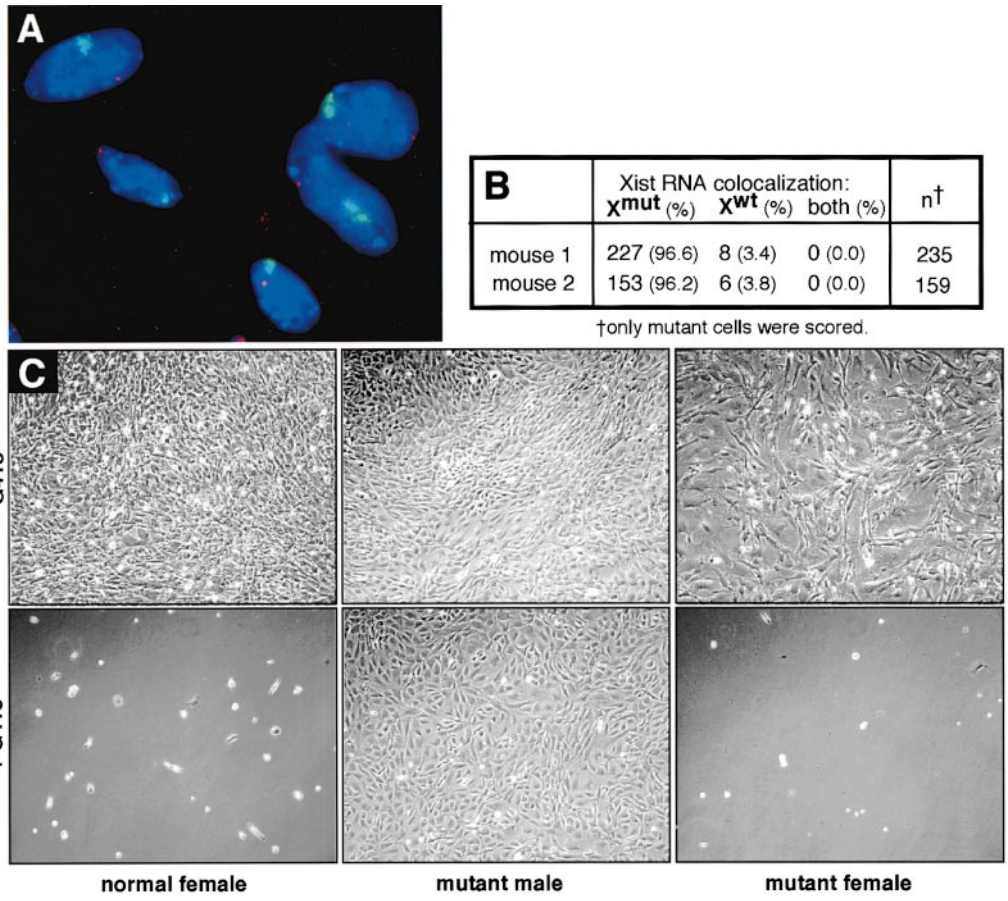

Figure 7. Nonrandom X Inactivation in Chimeric Mice

(A) RNA-DNA FISH of primary fibroblasts derived from mutant female ES cells. Primary fibroblasts were isolated from two chimeric mice. DNA FISH demonstrated that mouse 1 was ~60% chimeric, while mouse 2 was ~90% chimeric. A field of mutant cells from mouse 2 is shown. Allelic *Xist* expression was examined by two-color FISH which simultaneously detected *Xist* RNA (green; sense probes *b–d*, Figure 2) and the ΔCpG probe (red).

(B) Summary of allelic *Xist* expression in somatic cells isolated from two mice. Chimera cultures contained both normal and mutant cells. Only mutant cells were scored (mutant cells identified as those exhibiting only one ΔCpG signal).

(C) Primary fibroblasts were grown with or without 0.5 mg/ml G418 drug for 14 days.

antisense RNA throughout the 40 kb *Tsix* locus, consistent with loss of promoter function and supporting the idea that *Tsix* encodes a single 40 kb antisense transcript rather than multiple smaller RNAs. ΔCpG compromised X chromosome choice without disrupting counting or silencing. These results established that counting and choice are genetically separable. Although the 3.7 kb deletion did not affect counting, other *cis* elements within *Tsix* may be responsible for counting, a possibility that requires testing by additional *Tsix* knockouts.

Analysis of ΔCpG in XX female cells demonstrated that *Tsix* is required for the random nature of X chromosome choice. *Tsix* acts exclusively in *cis* and marks the future active X by blocking *Xist* accumulation. Interestingly, while *Tsix* has a repressive function in differentiating female cells, it serves no obvious function in undifferentiated cells. Although *Tsix* is normally expressed in undifferentiated cells, deleting *Tsix* does not lead to *Xist* accumulation on the mutant X despite a small elevation in *Xist* steady-state levels. This implicates other factors in addition to *Xist* and *Tsix* for initiation of X inactivation. One such "competence factor" is hypothesized later in this section.

Importantly, the present study does not discern whether the effects of ΔCpG are due to loss of *Tsix* RNA production or deletion of a critical DNA element such as a binding site for the putative blocking factor. If the DNA sequence were the crucial element, it becomes a philosophical debate as to whether the knockout phenotype is specifically related to the *Tsix* gene or to a 3′ regulatory element of *Xist*. Given that *Tsix* RNA deficiency resulted in elevation of steady-state *Xist* levels in undifferentiated cells and markedly skewed *Xist* upregulation in *cis*, we are tempted to speculate that the RNA itself is functional. *Tsix* RNA may negatively regulate *Xist* RNA stability by RNA duplex formation and targeting for degradation. Alternatively, *Tsix* RNA may mask chromosome-binding sites in *Xist* RNA and preclude "coating" of the chromosome.

A role for *Tsix* in regulating *Xist* and X chromosome choice is consistent with available genetic evidence. *Tsix* lies partially in the 65 kb region containing a putative

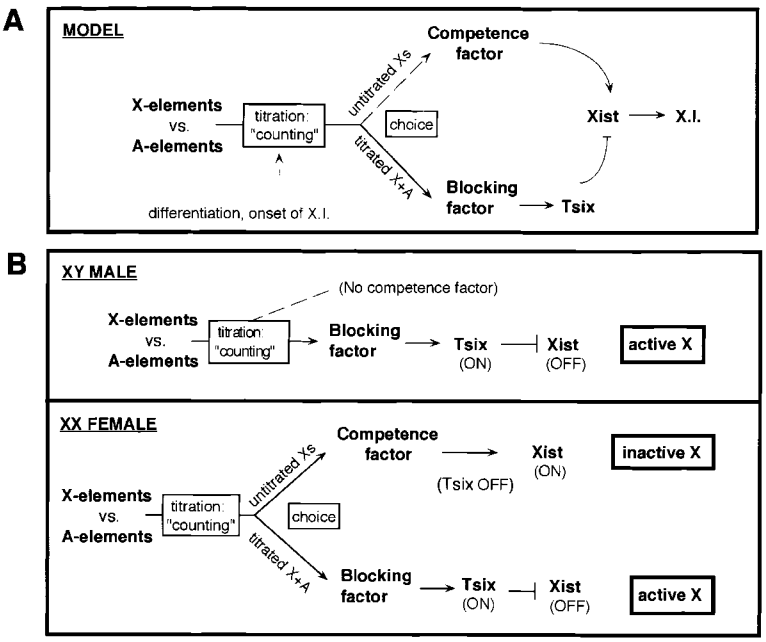

Figure 8. A Model for Counting and Choice

(A) Parallel pathways for choosing active and inactive Xs.

(B) Outcomes in XY male and XX female cells. Counting may occur before or during differentiation. X.I., X inactivation; X-elements, unspecified factors produced by X chromosome (X); A-elements, unspecified factors produced by autosomes (A).

Xist repressive element (Clerc and Avner, 1998) and resides completely within the 80 kb region believed to carry critical elements of *Xic* function, including those for X chromosome choice (Lee et al., 1999b). Transgenesis work has also shown that a 35 kb *Xist* cosmid lacking *Tsix* function expressed *Xist* ectopically and silenced a linked reporter gene (Herzing et al., 1997), a result supporting the conclusion that a *Tsix* deficiency leads to elevated *Xist* expression. Finally, ΔCpG deletes a CpG island in *Tsix* whose methylation status correlates inversely with *Xce* strength (Simmler et al., 1993; Courtier et al., 1995; Avner et al., 1998). X chromosomes carrying a strong *Xce* allele are hypomethylated in this 5′ region of *Tsix*, consistent with a role for *Tsix* expression in blocking high *Xist* expression. Since ΔCpG affects X chromosome choice, it will be important to determine in the future whether *Tsix* might be synonymous with the *Xce*.

Our conclusions also relate to those of a recent study (Marahrens et al., 1998) where analysis of an *Xist* knockout encompassing exons 1–5 suggested that a choosing element lies in this *Xist* region. Since exons 1–5 of *Xist* overlaps with *Tsix*, loss of choice in this mutation may reflect compromised *Tsix* rather than *Xist*. It is also possible that two elements—one at the 5′ end of *Tsix* and the other within *Xist*—are both necessary for choosing. Furthermore, in humans, a mutation in the *Xist* promoter has been associated with nonrandom X inactivation (Plenge et al., 1997). Therefore, multiple factors may act in epistatic and/or parallel pathways to control choice.

One aspect of the ΔCpG phenotype is strikingly different from that of the 65 kb knockout which truncates *Tsix* (Clerc and Avner, 1998). Both knockouts resulted in primary nonrandom X inactivation in XX cells. However, while ΔCpG had no effect in XY cells, the 65 kb deletion resulted in constitutive X inactivation even in mutant cells with only one intact X chromosome (interpreted as "X0"). Several differences may explain our contrasting results. First, ΔCpG covers a much smaller region than the 65 kb knockout. Indeed, the 65 kb deletion spans several genes besides *Tsix*, including all of the testes-specific gene *Tsx*, and the 3′ ends of *Xist* (exon 7) and brain-specific *Brx*. An additional repressive element for *Xist* may reside in the 65 kb region. A second difference is that the "X0" line was derived from the heterozygous 65 kb knockout XX ES line. It is possible that counting occurred just prior to cloning of the "X0" derivative. It is even possible that the original XX ES line was derived from an embryo that had already counted. A final difference is that the "X0" line underwent breakage and partial loss of the wild-type X (henceforth referred to as X^{Δ}), so that X^{Δ} lost the *Xic* locus but retained more proximal sequences; the X carrying the 65 kb deletion was unbroken (X^{65kb}). As such, the $X^{65kb}X^{\Delta}$ cell line is not equivalent to the $X^{\Delta CpG}Y$ cell line created here. By carrying fragments of two X chromosomes, $X^{65kb}X^{\Delta}$ may be more genetically similar to female than male cells; therefore, $X^{65kb}X^{\Delta}$ may be competent to undergo X inactivation due to the presence of as yet unidentified "competence factors."

The concept of a competence factor is supported by the key observation that X inactivation does not initiate in undifferentiated mutant female cells and in differentiating mutant male cells. They point to the existence of a second pathway of *Xist* regulation that is independent of *Tsix* or the ΔCpG sequence. To unify available genetic data, we propose that *Xist* is regulated in parallel pathways by positive and negative factors (Figure 8). Our model postulates that cells can produce two factors, a "blocking factor" (negative) and a "competence factor" (positive). The blocking factor marks the future active X by blocking the *Xic*. The blocking factor is a complex of X-linked and autosomal factors present in a stoichiometric ratio of one X to one diploid set of autosomes. Because the blocking factor is limiting, only one X remains active per diploid genome. The effects of ΔCpG argue that the blocking factor acts through *Tsix*.

The competence factor is required to initiate X inactivation on the future inactive X by upregulating *Xist*. Empirically, this positive factor is produced only when there is more than one X per diploid genome, because it is absent in X0 and XY but is present in XX, XXX, and XXXX cells. Since the autosomal content is identical, the critical factor must come from additional X chromosomes. We propose that the competence factor is made up of X-linked factors (perhaps the same as those in the blocking factor), but represent those which are not titrated by autosomal factors. Thus, XY cells produce no competence factor (only one X), XX cells produce one competence factor (one untitrated X), XXX diploid cells produce two (two untitrated Xs), and XXXX diploid cells produce three (three untitrated Xs).

This model is consistent with conclusions derived from various genetic studies. Others have also postulated positive elements controlling the choice of future inactive X (Marahrens et al., 1998). The hypothesized requirement for a competence factor explains why $X^{\Delta CpGY}$ male cells do not initiate X inactivation despite lacking *Tsix*. In contrast, the $X^{65kb}X^{\Delta}$ female cells (Clerc and Avner, 1998) initiate X inactivation, possibly because the X^{Δ} chromosome may retain elements for competence factor production. Specific aspects of our model will require genetic testing in the future. Recent progress in defining *Xic* sequence requirements and the establishment of *Tsix* as a genetic regulator should further facilitate dissection of the X inactivation cascade.

Experimental Procedures

Cell Lines, Culture, and Derivation of Mice

To generate karyotypically stable 40XX female ES lines, limiting dilution was performed on the mosaic 40XX/39X0 female cell line, EL16 (Lee et al., 1999a; E. Li, unpublished data). The 40XX subclone, 16.7, stably transmitted two X chromosomes for over 40 doubling times in culture (>90%, 40XX). Allele-specific genotyping revealed one X each of 129 and *M. castaneus* origins. The male ES line (J1, 40XY) has been described (Li et al., 1992). ES cells were maintained in 500 U/ml LIF, DME, and 15% FCS. EB were differentiated by suspension culture for 4 days without LIF and maintained thereafter under adherent conditions (Martin and Evans, 1975). Chimeric mice were generated from knockout ES cells by standard injection into C57BL/6 blastocysts (Papaioannou and Johnson, 1993). Primary fibroblasts were obtained from day 13.5 embryos or adult ear by culture in DME + 10% FCS. In tests of G418 resistance, 500 μg/ml of drug (active fraction) was added to test plates on the day indicated, and drug-free cultures were grown in parallel.

Targeted Deletion of *Tsix*

To create the targeting vector, a 2 kb BamHI-MluI fragment (+10.7 to +12.7 kb downstream of *Xist* exon 6) was inserted into the SalI cloning site of pLNTK (Gorman et al., 1996), a targeting vector which carries a *Pgk1* promoter-driven neomycin-resistance casette with flanking loxP sites and an HSV-thymidine kinase gene. Then a 7.7 kb SacI-BamHI fragment (+16.4 kb to +24.1 kb downstream of *Xist* exon 6) was inserted into the XhoI cloning site. All cloned sequences were of 129 origin. To generate knockout cell lines, 3×10^7 ES cells were electroporated (240 V., 500 μF, BioRad GenePulser) with 40 μg of linearized targeting construct, double drug selection (300 μg/ml G418, 2 μM gancyclovir) was begun at 24 hr, and resistant colonies were picked after 8 days (Wurst and Joyner, 1993). The targeting frequency was 8/106 in J1 and 3/150 in 16.7. To remove the *neo* cassette by Cre-mediated recombination at flanking loxP sites, ES cells were transiently transfected with pMC-CreN and selected as described (Torres and Kuhn, 1997).

FISH

Detailed methods for RNA and DNA FISH have been described (Lawrence et al., 1989; Trask, 1991; Panning and Jaenisch, 1996). All samples were fixed in 4% paraformaldehyde for 10 min at room temperature. Day 0 to 6 EB were dispersed by trypsinization and cytospun onto glass slides prior to fixation. Day 11 EB and mouse fibroblasts were grown directly on chamber slides and fixed in situ after Triton X-100 extraction (Lawrence et al., 1989). For RNA FISH, samples were not denatured prior to hybridization. For simultaneous RNA-DNA FISH, samples were denatured for 10 min at 80°C in 70% formamide, 2× SSC. Strand-specific probes were generated by riboprobe synthesis. *Xist*/*Tsix* sequences were cloned into pGEM11 and linearized by restriction digestion at sites within 0.5–1.0 kb of SP6 or T7 promoters. Standard SP6 and T7 transcription reactions (Promega) were performed for 1 hr in the presence of 0.5 mM each of ATP, CTP, GTP, and one of the following: fluorescein-12-UTP, biotin-16-UTP, or digoxigenin-11-UTP label (Boehringer Mannheim). Probes were treated with 1 U of RQ1 DNAse I per microgram of probe for 15 min, extracted with phenol:chloroform, precipitated, and resuspended to a final concentration of 2 ng/μl. All hybridizations proceeded overnight at 42°C. Digoxigenin- and biotin-labeled probes were indirectly visualized with a rhodamine-conjugated anti-digoxigenin antibody (Boehringer Mannheim) and avidin-Texas red (Vector). Detection of *Xist* required signal amplification with anti-fluorescein antibodies (Boehringer Mannheim) or NEN's TSA-Direct (GreenFISH). Probes *a*–*c* (Figure 2) are described in relation to +1 bp of the *Xist* cDNA: *a* (−5,216 to −1,652), *b* (6,948–9,425), *c* (10,992–15,917). Probe *d* covers 2,301–5,251 and *e* covers 10,733–15,047 bp downstream of *Xist* exon 6. *Pgk1* was detected using pCAB17, a 17 kb genomic clone. *Mecp2* was detected by pKpn12, a 12 kb genomic plasmid.

RT–PCR

Strand-specific RT–PCR was performed using 30 cycles of amplification as previously described (Lee et al., 1999a). +RT and −RT reactions were included for all samples. The following primer sequences are described in relation to +1 bp of the *Xist* cDNA, with "s" and "as" denoting sense and antisense primers: 1s (−3116 to −3096), 1as (−2964 to −2984), 2s (−1033 to −1013), 2as (−794 to −814), 3s (272–294), 3as (775–755), 4s (13,177–13200), 4as (13,428–13,401). 5s is positioned at bp 9,823–9,842 and 5as at bp 10,181–10,161 downstream of *Xist* exon 6. *Rrm2* cDNA was amplified by Rrm2A and Rrm2C (Lee and Jaenisch, 1997). For allele- and strand-specific quantitative RT–PCR of *Xist*, first-strand cDNA was synthesized from 1 μg of total RNA using primer 3as at 52°C for 1 hr and amplified by ^{32}P end-labeled primer 3s and cold primer 3as. To enable quantitation, standard curves were generated for allele-specific RT–PCR, indicating exponential amplification between 15–28 cycles; 24 cycles was selected and *Rrm2* (Rrm2A+Rrm2C yields a 360 bp fragment) served as internal standard in each reaction. PCR products were purified through Qiagen QIAquick columns and digested with NcoI. NcoI cuts once in the 3s-3as PCR product, revealing a labeled fragment of 224 bases from *M. castaneus* and 227 bases from 129 (Hendrich et al., 1993; Carrel et al., 1996). Products were resolved on a 6% polyacrylamide/7.5 M urea gel and quantitated by phosphorimaging (Molecular Dynamics).

Acknowledgments

We thank D. Warshawsky for assistance in cloning the knockout construct, N. Stavropoulos for identifying the MnlI *Tsix* polymorphism, B. Seed for use of the animal facility, and T. Budzinski and C. Cassie for technical assistance. We also thank J. Manis for pLNTK, R. Chen for pKpn12, W. McBurney for pCAB17, and J. E. Kirby, N. Stavropoulos, J. Conaty, and B. Seed for critical comments on the manuscript. N. L. is a mouse specialist at the DMB/MGH Mouse Facility. This work was funded by National Institutes of Health (RO1 GM58839A01), March of Dimes (Basil O'Connor Starter Scholar Fund 5FY99-0162), and Hoechst awards to J. T. L.

Received July 12, 1999; revised September 1, 1999.

References

Avner, P., Prissette, M., Arnaud, D., Courtier, B., Cecchi, C., and Heard, E. (1998). Molecular correlates of the murine *Xce* locus. Genet. Res. Camb. *72*, 217–224.

Brockdorff, N. (1998). The role of *Xist* in X-inactivation. Curr. Opin. Genet. Dev. *8*, 328–333.

Brockdorff, N., Ashworth, A., Kay, G.F., McCabe, V.M., Norris, D.P., Cooper, P.J., Swift, S., and Rastan, S. (1992). The product of the mouse *Xist* gene is a 15 kb inactive X-specific transcript containing no conserved ORF and located in the nucleus. Cell *71*, 515–526.

Brown, C.J., Hendrich, B.D., Rupert, J.L., Lafreniere, R.G., Xing, Y., Lawrence, J., and Willard, H.F. (1992). The human *XIST* gene: analysis of a 17 kb inactive X-specific RNA that contains conserved repeats and is highly localized within the nucleus. Cell *71*, 527–542.

Carrel, L., Hunt, P.A., and Willard, H. (1996). Tissue and lineage-specific variation in inactive X chromosome expression of the murine *Smcx* gene. Hum. Mol. Genet. *5*, 1361–1366.

Cattanach, B.M., and Papworth, D. (1981). Controlling elements in the mouse. V. Linkage tests with X-linked genes. Genet. Res. Camb. *38*, 57–70.

Cattanach, B.M., and Rasberry, C. (1994). Identification of the *Mus castaneus Xce* allele. Mouse Genome *92*, 114.

Clemson, C.M., McNeil, J.A., Willard, H., and Lawrence, J.B. (1996). *XIST* RNA paints the inactive X chromosome at interphase: evidence for a novel RNA involved in nuclear/chromosome structure. J. Cell Biol. *132*, 259–275.

Clerc, P., and Avner, P. (1998). Role of the region 3′ to *Xist* in the counting process of X-chromosome inactivation. Nat. Genet. *19*, 249–253.

Cooper, D.W., VandeBerg, J.L., Sharman, G.B., and Poole, W.E. (1971). Phosphoglycerate kinase polymorphism in kangaroos provides further evidence for paternal X inactivation. Nat. New Biol. *230*, 155–157.

Courtier, B., Heard, E., and Avner, P. (1995). *Xce* haplotypes show modified methylation in a region of the active X chromosome lying 3′ to *Xist*. Proc. Natl. Acad. Sci. USA *92*, 3531–3535.

Drews, R., Blecher, S.R., Owen, D.A., and Ohno, S. (1974). Genetically directed preferential X-activation seen in mice. Cell *1*, 3–8.

Eicher, E.M. (1970). X-autosome translocations in the mouse: total inactivation versus partial inactivation of the X chromosome. Adv. Genet. *15*, 175–259.

Epstein, C., Smith, S., Travis, B., and Tucker, G. (1978). Both X-chromosomes function before visible X-chromosome inactivation in female mouse embryos. Nature *274*, 500–503.

Gartler, S.M., and Riggs, A.D. (1983). Mammalian X-chromosome inactivation. Annu. Rev. Genet. *17*, 155–190.

Gorman, J.R., Stoep, N.v.d., Monroe, R., Cogne, M., Davidson, L., and Alt, F.W. (1996). The Ig(kappa) enhancer influences the ratio of Ig(kappa) versus Ig(lambda) B lymphocytes. Immunity *5*, 241–252.

Hendrich, B.D., Brown, C.J., and Willard, H.F. (1993). Evolutionary conservation of possible functional domains of the human and murine *Xist* genes. Hum. Mol. Genet. *2*, 663–672.

Herzing, L.B.K., Romer, J.T., Horn, J.M., and Ashworth, A. (1997). *Xist* has properties of the X-chromosome inactivation centre. Nature *386*, 272–275.

Kratzer, P.G., and Gartler, S.M. (1978). HGPRT activity changes in preimplantation mouse embryos. Nature *274*, 503–504.

Lawrence, J.B., Singer, R.H., and Marselle, L.M. (1989). Highly localized tracks of specific transcripts within interphase nuclei visualized by in situ hybridization. Cell *57*, 493–502.

Lee, J.T., and Jaenisch, R. (1997). Long-range cis effects of ectopic X-inactivation centres on a mouse autosome. Nature *386*, 275–279.

Lee, J.T., Strauss, W.M., Dausman, J.A., and Jaenisch, R. (1996). A 450 kb transgene displays properties of the mammalian X-inactivation center. Cell *86*, 83–94.

Lee, J.T., Davidow, L.S., and Warshawsky, D. (1999a). *Tsix*, a gene antisense to *Xist* at the X-inactivation center. Nat. Genet. *21*, 400–404.

Lee, J.T., Lu, N.F., and Han, Y. (1999b). Genetic analysis of the mouse X-inactivation center reveals an 80kb multifunction domain. Proc. Natl. Acad. Sci. USA *96*, 3836–3841.

Li, E., Bestor, T.H., and Jaenisch, R. (1992). Targeted mutation of the DNA methyltransferase gene results in embryonic lethality. Cell *69*, 915–926.

Lyon, M.F. (1961). Gene action in the X-chromosome of the mouse (*Mus musculus* L.). Nature *190*, 372–373.

Lyon, M.F. (1971). Possible mechanisms of X chromosome inactivation. Nat. New Biol. *232*, 229–232.

Lyon, M.F. (1972). X-chromosome inactivation and developmental patterns in mammals. Biol. Rev. *47*, 1–35.

Lyon, M.F. (1996). Pinpointing the centre. Nature *379*, 116–117.

Marahrens, Y., Loring, J., and Jaenisch, R. (1998). Role of the *Xist* gene in X chromosome choosing. Cell *92*, 657–664.

Martin, G.R., and Evans, M.J. (1975). Differentiation of clonal lines of teratocarcinoma cells: formation of embryoid bodies in vitro. Proc. Natl. Acad. Sci. USA *72*, 1441–1445.

McMahon, A., Fosten, M., and Monk, M. (1983). X-chromosome inactivation mosaicism in the three germ layers and the germ line of the mouse embryo. J. Embryol. Exp. Morphol. *74*, 207–220.

Monk, M., and Harper, M.I. (1979). Sequential X chromosome inactivation coupled with cellular differentiation in early mouse embryos. Nature *281*, 311–313.

Ohno, S. (1969). Evolution of sex chromosomes in mammals. Annu. Rev. Genet. *3*, 495–524.

Panning, B., and Jaenisch, R. (1996). DNA hypomethylation can activate *Xist* expression and silence X-linked genes. Genes Dev. *10*, 1991–2002.

Panning, B., Dausman, J., and Jaenisch, R. (1997). X chromosome inactivation is mediated by *Xist* RNA stabilization. Cell *90*, 907–916.

Papaioannou, V., and Johnson, R. (1993). Production of chimeras and genetically defined offspring from targeted ES cells. In Gene Targeting: A Practical Approach, A.L. Joyner, ed. (Oxford, UK: Oxford University Press), pp. 107–146.

Penny, G.D., Kay, G.F., Sheardown, S.A., Rastan, S., and Brockdorff, N. (1996). Requirement for *Xist* in X chromosome inactivation. Nature *379*, 131–137.

Plenge, R.M., Hendrich, B.D., Schwartz, C., Arena, J.F., Naumova, A., Sapienza, C., Winter, R.M., and Willard, H.F. (1997). A promoter mutation in the *XIST* gene in two unrelated families with skewed X-chromosome inactivation. Nat. Genet. *17*, 353–356.

Rastan, S., and Brown, S.D.M. (1990). The search for the mouse X-chromosome inactivation centre. Genet. Res. Camb. *56*, 99–106.

Rastan, S., and Robertson, E.J. (1985). X-chromosome deletions in embryo-derived (EK) cell lines associated with lack of X-chromosome inactivation. J. Embryol. Exp. Morphol. *90*, 379–388.

Sheardown, S.A., Duthie, S.M., Johnston, C.M., Newall, A.E.T., Formstone, E.J., Arkell, R.M., Nesterova, T.B., Alghisi, G.-C., Rastan, S., and Brockdorff, N. (1997). Stabilization of *Xist* RNA mediate initiation of X chromosome inactivation. Cell *91*, 99–107.

Simmler, M.-C., Cattanach, B.M., Rasberry, C., Rougeulle, C., and Avner, P. (1993). Mapping the murine *Xce* locus with (CA)n repeats. Mamm. Genome *4*, 523–530.

Takagi, N., and Sasaki, M. (1975). Preferential inactivation of the paternally derived X-chromosome in the extraembryonic membranes of the mouse. Nature *256*, 640–642.

Torres, R.M., and Kuhn, R. (1997). Laboratory Protocols for Conditional Gene Targeting (Oxford: Oxford University Press).

Trask, B.J. (1991). Fluorescence in situ hybridization. Trends Genet. *7*, 149–154.

Wurst, W., and Joyner, A.L. (1993). Production of targeted embryonic stem cell clones. In Gene Targeting: A Practical Approach, A.L. Joyner, ed. (Oxford: IRL Press), pp. 33–61.